IEEE Robotics and Automation Letters (RAL) paper presented at
2024 IEEE/RSJ International Conference on Intelligent Robots and Systems (IROS)
October 14-18, 2024. Abu Dhabi, UAE

Self-sensing Origami-inspired Soft Twisting Actuators and Its Application in Soft Robots

Yang Yang, *Senior Member, IEEE,* Shaoyang Yan, Yuan Xie, Yuchao Wang, Jia Liu, Yunquan Li, *Member, IEEE* and Jianshu Zhou, *Member, IEEE*

***Abstract*— The good compliance of soft robots provides a reliable safety environment for human-robot interaction; however, it also creates challenges for adding sensors to soft robots. In this letter, we propose a self-sensing origami-inspired soft twisting actuator. The actuator is designed based on the structure of origami, enabling the compound motion of twist and contraction. The position sensor made from flexible fabric material is integrated in the soft actuator body. With twisting angle feedback, the self-sensing twisting actuator can not only provide expected motion but also acquire additional environment information based on real-time sensing. This paper discusses the design, fabrication, and experimental validation of proposed self-sensing twisting actuator. Based on the self-sensing twisting actuator, a soft gripper, a soft robotic arm, and a soft hexapod robot, all vacuum-powered, are designed and prototyped to validate their performance. The proposed soft actuator has great potential for applications in scenarios that require self-sensing information and closed-loop control.**

***Index Terms*—Soft actuator, origami-inspired actuator, soft sensor, flexible fabric material.**

I. Introduction

In recent years, soft robots constructed from flexible materials have attracted significant attention in the field of robotics due to their excellent compliance and adaptability [1]. Traditional rigid robots focus on force, speed, and precision [2] but are limited by their rigid structures and joints, adding lots of computation and control burden for operations in unstructured environments. The inherent compliance of soft robots provides an effective solution to address this challenge [3]. The applications of soft robots in scenarios such as soft robotic arms [4], grippers [5], and medical devices [6] have demonstrated the potential of soft robots in everyday environment and human-robot interaction. In addition, innovations in actuation methods, such as shape memory polymer [7], [8], shape memory alloy [9], electroactive polymer [10], and twisted-coiled actuators [11], have further expanded the application scenarios of soft robots. Among them, soft pneumatic actuators are widely applied due to their safety, lightweight, and ability to provide continuous and flexible motion, rather than being restricted by rigid structures. Except positive-pressure soft pneumatic actuators, vacuum driven soft pneumatic actuators have been reported in several studies due to their implicitly fail-safe operation [12-14].

The inherent compliance and conformability of soft robots, along with the flexibility of the construction materials, make integrating sensors to soft robots a challenge. Commercially available sensors, such as encoders, strain gauges, and inertial measurement units (IMUs) are not suitable for soft robots as they may impede the inherent compliance of soft robots. Compared to the expected characteristics of sensors for traditional rigid robots, soft robots require additional features [15]. Sensors designed for soft robots should have a comparable low modulus to match the underlying structure. Attaching sensors to the robot body should not impart any additional, noticeable impedance changes to the entire structure. The fabrication materials of sensors should possess stretchability, similar to other components of the soft robot [16]. A number of methods for embedding sensors in soft actuators to achieve self-sensing are reported, such as integrating hybrid optical fiber to measure the bending deformation and contact force of soft pneumatic grippers [17], using conductive elastomers with piezoresistive effects to measure pressure and position of soft fingers [18], applying resistive fabric to measure length changes in the contractile actuator [19], and so on. Among them, sensors based on flexible fabric piezoresistive materials offer a promising direction to address the challenges of soft robot sensing.

Sensors based on flexible fabric piezoresistive materials belong to the category of resistive sensors. They are easy to manufacture, and cost-effectiveness is quite high. In addition, the use of flexible fabric piezoresistive materials can simplify the process of integrating sensors into a soft robot, reducing the time-consuming process, and the embedding of flexible

Manuscript received: September 26, 2023; Revised: November 17, 2023; Accepted: December 12, 2023. This paper was recommended for publication by Editor Yong-Lae Park upon evaluation of the Associate Editor and Reviewers' comments.

This research was partly supported by the National Natural Science Foundation of China (Grant No. 52005269), the Research Project of State Key Laboratory of Mechanical System and Vibration MSV202319, and the Research Grants Council of Hong Kong (GRF No. 14207423) (*Corresponding authors: Yang Yang, Jianshu Zhou*)

Yang Yang, Shaoyang Yan, Yuan Xie, Yuchao Wang and Jia Liu are with the School of Automation, Nanjing University of Information Science and Technology, Nanjing 210044, Jiangsu, China, the Jiangsu Province Engineering Research Center of Intelligent Meteorological Exploration Robot and the Jiangsu Collaborative Innovation Center of Atmospheric Environment and Equipment Technology (CICAEET) (e-mail: meyang@nuist.edu.cn; 202212570005@nuist.edu.cn; 20211249100@nuist.edu.cn; wychihi@foxmail.com; 001930@nuist.edu.cn).

Yunquan Li is with the Shien-Ming Wu School of Intelligent Engineering, South China University of Technology, Panyu District, Guangzhou, Guangdong, China (email: yunquanli@scut.edu.cn).

Jianshu Zhou is with the Department of Mechanical and Automation Engineering, the Chinese University of Hong Kong, Hong Kong, and the Hong Kong Center for Logistics Robotics, Hong Kong (email: jianshuzhou@cuhk.edu.hk).

Digital Object Identifier (DOI): see top of this page.

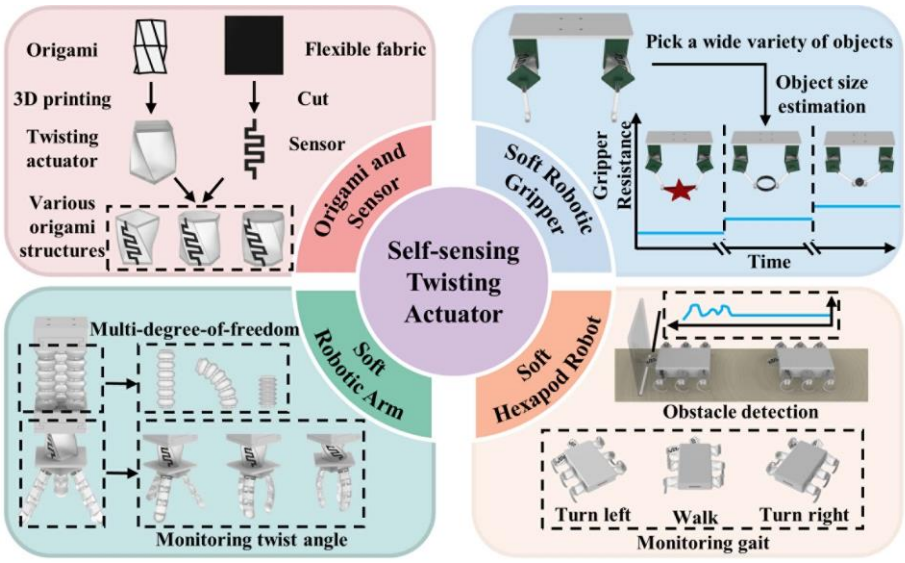

Fig. 1. Proposed self-sensing twisting actuator and its application in soft robots.

fabric piezoresistive materials does not alter the inherent compliance of the soft robot. Hence, embedding flexible fabric sensors into soft pneumatic actuators to achieve self-sensing in soft actuators is a logical expectation. Origami-inspired structures have been proven to be an effective solution for reducing the response time of soft pneumatic actuators [20]. Soft pneumatic actuators based on origami-inspired structures exhibit unique bistability characteristic that promote deformation and reduce the response time of the actuators. The origami-inspired actuator can function as a twisting actuator and be applied in multiple scenarios [21-24]. However, the reported origami-inspired twisting actuators still lack the embedded soft position sensors to provide real-time twisting angle information during free motion or interaction with environment for self-monitoring or closed-loop control in sophisticated operations.

In this letter, we present a self-sensing origami-inspired soft twisting actuator (Figure 1). Flexible fabric piezoresistive materials are used as position sensors for soft actuators while 3D-printed vacuum-powered origami structures are used as pneumatic actuators. Flexible fabric materials can be combined with various origami-structured actuators to achieve self-sensing capabilities. By adjusting the magnitude of the input vacuum pressure, the soft twisting actuator can twist to the desired angle, causing changes in the resistance of the flexible fabric sensor. Therefore, the resistance change can be used to reflect the real-time twisting angle of the soft twisting actuator. This makes it easy to control the behavior of the proposed soft actuator. Based on the proposed self-sensing twisting actuator, we have designed and fabricated a soft gripper, a soft robotic arm, and a soft hexapod robot, all of which are actuated by vacuum pressure and can obtain position information and other environmental information through self-sensing. Moreover, closed-loop control can be conducted based on the actuator's sensory feedback.

The paper is organized as follows: section II describes the design, fabrication, and experimental characterization of the self-sensing twisting actuator. Section III describes the application of the self-sensing twisting actuator to a soft robotic gripper, a soft robotic arm, and a soft hexapod robot in order to demonstrate its effectiveness. Conclusions and discussions are given in Section IV.

II. DESIGN AND MODELING OF THE SELF-SENSING TWISTING ACTUATOR

A. Actuator Design

The actuator that adopts the origami structure can achieve the compound motion of twist and contraction when actuated by vacuum pressure, as shown in Figure 2(a). As shown in Figure 2(b), the actuator is in the actuated state. The twisting actuator is soft and consists of a top surface, four curved surfaces, and a bottom surface (Figure 2(c)). The bottom surface features a circle hole for inserting a silicone hose. The thickness of the top and bottom surfaces is 1.8mm thicker than the thickness of the curved surface (1.2mm) to ensure that the top and bottom surfaces are not recessed when the actuator is actuated. The twisting direction of the actuator is consistent with the direction of the slanted sides. The initial height of the twisting actuator is H_0, the side length is D, and the initial angle between the top and bottom surfaces is β (Fig 2(d)).

Figure 2(e) shows the relationship between the pressure and the angle change. The twisting angle increases with the increase in pressure, and when the pressure is at -93 kPa, the twisting angle can reach 60°. When the pressure increases to -40~-45 kPa, the twisting angle of the actuator increases suddenly, as shown in the shadowed area in 2(e). This is because the actuator approaches an unstable negative stiffness state at this stage, leading to a sudden increase in acceleration and deformation, resulting in the phenomenon of snap-through [25-28]. This phenomenon causes the deformation of the actuator to be uncontrollable within a certain range, making it challenging for the closed-loop control system to accurately predict and adjust. Experiments were conducted by varying the initial height H_0 and the initial angle β to improve this phenomenon. All samples have a bottom area of 30*30mm^2.

As the initial angle β increases from 15° to 45°, there is no significant change in the maximum twisting angle of the actuator. For $\beta > 35°$, the snap-through behavior of the actuator essentially disappears (Figure 2(e)). As shown in Figure 2(f),

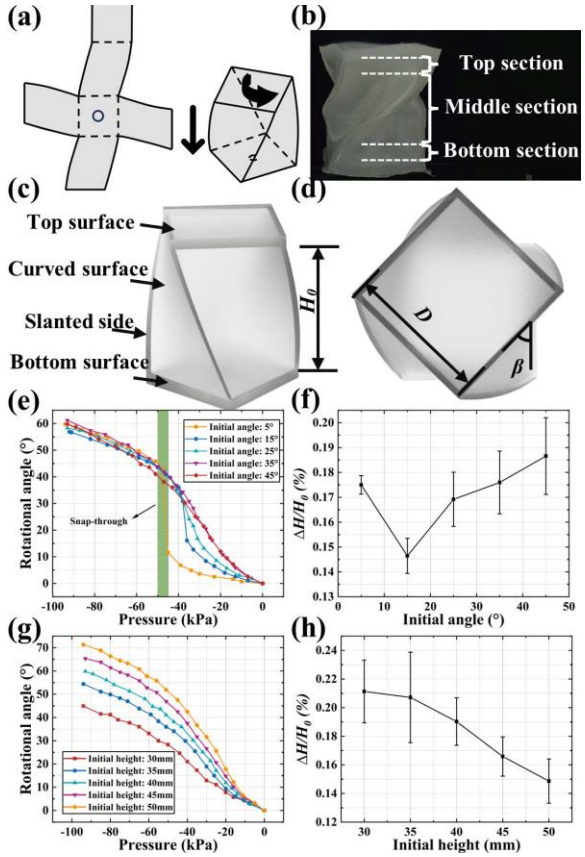

Fig. 2. Vacuum-powered twisting actuator based on origami structure and its characteristics. (a) Origami Structure. (b) Twisting actuator being actuated. (c) The schematic of the twisting actuator structure. H_0 is the initial height. (d) Top view of the twisting actuator. β is the initial angle between the top and bottom surfaces. D is the initial length of the side. (e) The relationship between pressure and rotational angle with different initial angles β. (f) Relative height ($\Delta H/H_0$) change with different initial angles β. (g) The relationship between pressure and rotational angle with different initial heights H_0. (h) Relative height change($\Delta H/H_0$) with different initial heights H_0.

the initial angle β has a relatively small impact on the relative height change ($\Delta H/H_0$). Similarly, we gradually increased H_0 from 30mm to 50mm to study the impact of the initial height H_0 of the twisting actuator. As shown in Figure 2(g), the maximum twisting angle of the actuator increases with the increase in the initial height H_0. For H_0 > 30mm, as H_0 increases, the relative height change ($\Delta H/H_0$) continuously decreases (Figure 2(h)). This is because when the twisting actuator is actuated, the top and bottom sections have a larger contraction and smaller angle change compared to the middle section. The length of the top and bottom sections remains constant, while the middle section increases with the increase in the initial height H_0.

The twisting actuator was manufactured by a 3D printer (KP3S, KINGROON, China) and Thermoplastic Elastomer (TPE) material. To avoid secondary processing, we printed the twisting actuator as a single unit. A sturdy yet thin wall is conducive to promoting the twisting and contraction of the twisting actuator. Considering a printer nozzle diameter of 0.4mm, we set the wall thickness to 1.2mm. Simultaneously, we set the extrusion rate of the nozzle to 115% and the infill density to 100% to enhance the airtightness of the twisting actuator.

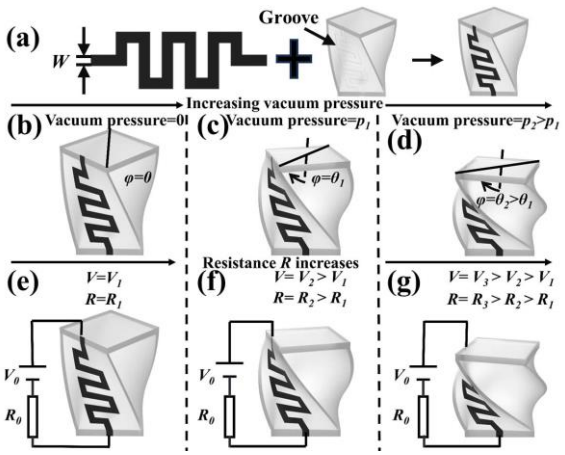

Fig. 3. Working principle of the sensor. (a) Design of the position sensor. The width is W. (b) The twisting actuator is in the initial state. (c) The twisting actuator is actuated using vacuum pressure with a twisting angle of φ. (d) The twisting angle φ increases as the vacuum pressure increases. (e)-(g) As the twisting angle increases, the degree of depression of the curved surface increases, leading to an increase in the load on the position sensor, which results in a change in the resistivity of the material and a change in the resistance value.

B. Design of the Position Sensor

In this study, a low-cost flexible fabric material named "Velostat (3M, USA)" is used for position sensing. Velostat is made of opaque and conductive material, carbon-impregnated polyolefin. When the load is applied, the conductive carbon particles in the fabric material show micro-Brownian motion [29], [30] and the distance between the carbon particles are changed, resulting in the change of the resistivity of the material, and the change of resistance value. This feature is used to sense the actuator's twisting angle.

The Velostat is cut into the shape shown in Figure 3(a) and attached to the groove on the curved surface of the twisting actuator using silicone adhesive. The shape of the position sensor is designed to maximize contact with the groove of the curved surface, enhancing its ability to perceive and adapt to changes in the curved surface during deformation. This facilitates precise measurement of the twisting angle.

When vacuum pressure is applied, the actuator realizes twisting motion (Figure 3(b)-(d)). As the twisting angle increases, the degree of depression of the curved surface increases, leading to an increase in the load on the position sensor. This results in a change in the resistivity of the material and a change in the measured resistance value, which is related to the twisting angle of the actuator (Figure 3(e)-(g)). Various technologies exist to measure the resistance of Velostat in real time, allowing this material to be used as a sensor for the actuator.

C. Experimental study of the Self-sensing Twisting Actuator

To validate the ability to perceive the twisting angle through measurement of the sensor's resistance, an experimental platform is set up as shown in Figure 4(a). The bottom surface of the test sample is fixed on the experimental platform, so that the self-sensing twisting actuator can only make a compound movement of twist and contraction. The actuator is actuated by a vacuum pump, which is connected to a pressure regulator to obtain a pressure range from 0 to -93kPa.

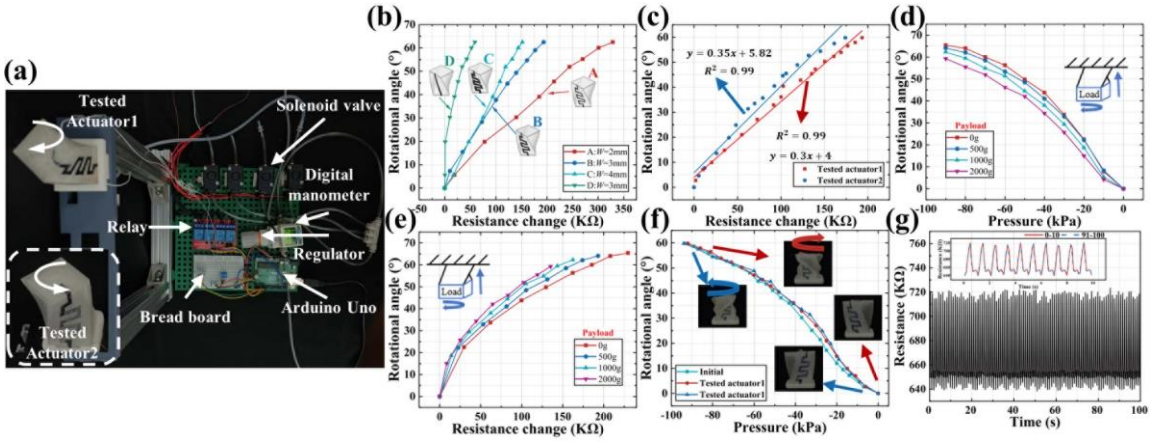

Fig. 4. Sensor characterization. (a) Experimental platform. (b) The relationship between resistance changes and rotational angle for position sensors of different shapes and sizes. (c) Experimental results of position sensor characterization. The sensor is selected as sample B. (d) and (e) The impact of different payloads on the characteristics of the self-sensing twisting actuator. (f) The impact of adding a sensor on the characteristics of the actuator. (g) Repeatability test of the self-sensing actuator. The inset figure displays the resistance for the first 10 cycles and the last 10 cycles.

The output pressure is calibrated with a digital manometer. To control the on-off state of the pneumatic circuit, relays are employed to control the solenoid valves. The twisting motion of the actuator is captured by a camera, and the twisting angle is later measured using a motion capture software (Kinovea). The two ends of the sensor are connected to wires through terminals, and wires are connected to an Arduino UNO controller to measure and record the resistance value. The sampling frequency is set at 10Hz. The resistance value is measured using a voltage divider method and processed with mean value filtering to reduce interference.

Firstly, the impact of the shape and size of the sensor on the sensing performance is studied, and the results are presented in Figure 4(b). Samples A, B and C all have meander sensor structure but with different width W while sensor in Sample D is straight. As W decreases, the initial resistance of the sensor increases, leading to an increase in the resistance change of the sensor. Samples B and D have the same W, but the initial resistance of sample B is larger than that of sample D, which indicates that the meander structure can effectively increase the length of the sensor and thus increase the initial resistance. Samples C and D have similar initial resistance values, with a difference within 30KΩ. However, when reaching the maximum twisting angle, the resistance change for sample C is 152KΩ, which is much larger than 59KΩ of sample D. These results suggest that the meander structure facilitates better contact with the groove, enhancing the perception and adaptation to changes in the curved surface. To make a compromise between resistance variation range and linearity, we choose a sensor prototype with a meander structure and W of 3mm. The resistance variation with the twisting angle is shown in Figure 4(c). The initial resistance of Tested Actuator 1 is 450KΩ, and 400KΩ for Tested Actuator 2. Tested Actuator 1 can rotate clockwise and Tested Actuator 2 can rotate counterclockwise. By performing a linear fit on the experimental data points, a strong linear relationship is demonstrated, indicating that the resistance change of the position sensor can effectively perceive the twisting angle of the actuator, unaffected by the twisting direction.

Next, the impact of the payload on the performance of the self-sensing twisting actuator is also investigated. We measured the performance of the actuator under pressure ranging from 0 to -90 kPa and payload from 0 to 2000g. As shown in Figure 4(d), due to the need for a certain force to counteract the payload, the maximum twisting angle decreases with the increase of payload. In Figure 4(e), similarly, the resistance change of the position sensor decreases with the increase of payload.

In order to investigate the impact of embedded sensors on the performance of twisting actuators, three different actuators are tested including an initial actuator without a position sensor and the other two of the proposed Tested Actuator 1 and Tested Actuator 2 with position sensors and opposite twisting directions. As shown in Figure 4(f), three actuators exhibit the same trend of variation, this indicates that the deformation of the twisting actuator is not influenced by embedding the position sensor, meaning that adding the flexible fabric as a sensor to the soft actuator does not disrupt its inherent compliance.

As shown in Figure 4(g), we conduct repeatability test on the position sensor. At a pressure of -90kPa, cyclic tests are conducted at a frequency of 1 Hz for 100 cycles. The inset figure displays the resistance for the first 10 cycles and the last 10 cycles. The experimental results indicate that, over 100 cycles of testing, the relative change in resistance peak value is less than 5%, and the sensor shows good cyclic repeatability under continuous deformation.

III. SAMPLE APPLICATIONS

A. Soft Gripper

The proposed self-sensing twisting actuator is used to configure a soft gripper, as shown in Figure 5(a). When actuated, the self-sensing twisting actuator 1 rotates counterclockwise, and the self-sensing twisting actuator 2 rotates clockwise, causing the two soft fingers to get close for grasping objects. Cylinders of different lengths (30mm, 60mm, 90mm) are grasped and resistance changes of the two actuators' position sensors are recorded respectively to explore the ability of the gripper to sense the size of the object. As shown in Figure 5(b), the smaller the object size, the greater the

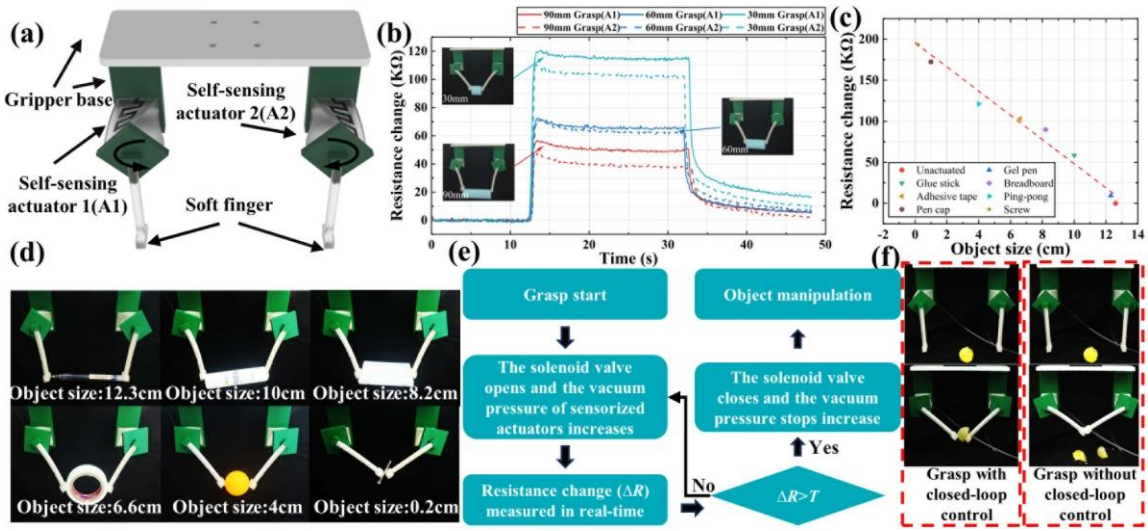

Fig. 5. Soft gripper. (a) Structural design of the gripper. (b) The corresponding resistance changes when the gripper grasps cylinders of different lengths. (c) and (d) Using the gripper to grasp objects of different sizes and recording the resistance value when the gripper touches the object and the object does not fall. (e) Closed-loop control diagram. (f) Using different actuation strategies to grasp an egg yolk, one successfully grasped, one damaged.

resistance change is observed in the position sensor. When grasping a 30mm cylinder, the resistance value of the sensor A1 can change up to 120 KΩ. After grasping the object (14s-32s), the relative standard deviation of the resistance changes in A1 is less than 4%, which also shows the stability of the embedded sensor. These results suggest that the soft gripper with proposed actuator can be used to estimate the size of grasped objects. Additionally, the self-sensing twisting actuators can also be used to detect whether an object is in contact with the gripper. If an object falls during transport, the resistance of the actuators will also change significantly.

As shown in Figure 5(d), the gripper is used to grasp objects of different sizes and the resistance value when the gripper touches the object till it does not fall is recorded. Based on the experimental results (Figure 5(c)), a closed-loop control logic is designed (Figure 5(e)). In order to measure the size of unknown objects, we have introduced visual sensing technology. However, it is important to emphasize that this technology is not intended for closed-loop control. After knowing the size of the object, the corresponding resistance value for that size is set as the threshold(T) in the control program. During the grasping process, the resistance change(ΔR) is measured in real-time. If ΔR is larger than T, the solenoid valve will close, and vacuum pressure of the sensorized actuators will stop increase. Otherwise, the actuators will continue to act and the measurement of ΔR also continues. To assess the effectiveness of this scheme, a delicate egg yolk is grasped and the results are shown in Figure 5(f). With closed-loop control, the egg yolk is successfully clipped up. Otherwise, the gripper may easily break the egg yolk during grasping. The gripper's grasping of a delicate tofu with and without closed-loop control can be seen in the Supplementary Video.

B. Soft Robotic Arm

The self-sensing twisting actuator can also be applied to develop a soft robotic arm. We construct a soft robotic arm using three bellow, one self-sensing twisting actuator as the wrist joint of the arm, three soft fingers, and multiple connecting structures, as shown in Figure 6(a). Each bellow has a separate vacuum channel, and by employing different actuating strategies to control the three bellows, the robotic arm can be bent to various angles. The three soft fingers make up the gripper, which is used for grasping and releasing objects. The self-sensing twisting actuator is used as a soft wrist, actuating the soft fingers to twist. The bellows, twisting actuator, and soft fingers are all actuated by vacuum pressure.

Firstly, performance of the soft robotic arm is demonstrated by using it to unscrew a bottle cap. As shown in Figure 6(b), the cap can be unscrewed by repeating the continuous motion of steps b1-b4. When the pressure is -93 kPa, unscrewing the bottle cap requires repeating the continuous motion of steps b1-b4 four times. When the pressure is -50 kPa, it requires repeating six times. At pressures of -93 kPa and -50 kPa, the corresponding resistance changes are approximately 175 KΩ and 100 KΩ. Based on the relationship between resistance change and twisting angle in Figure 4(c), a single twisting angle is approximately 60° and 40° for -93 kPa and -50 kPa. In the next experiment, the robotic arm can install a light bulb by repeating the continuous motion of steps b4-b1 (Figure 6(c)). These results indicate that we can monitor the rotation frequency and twisting angle of the robotic arm in real-time by measuring the resistance.

Closed-loop control of the robotic arm is also realized based on the relationship between the actuator's twisting angle and the sensor's resistance, as shown in Figure 6(d) and 6(e). Firstly, image of the prism and groove is captured using the camera placed on the top of the platform. Through edge recognition and feature extraction, the angular deviation between the groove and prism is identified (Figure 6(d)(i)). Subsequently, in the control program, the resistance value corresponding to the angular deviation is set as threshold T. Afterwards, the soft fingers are actuated to grasp the prism, and the arm is moved towards the groove using a stepper motor. ΔR is measured in real-time. If ΔR is larger than T, the solenoid value will close, and the vacuum pressure of the sensorized actuator will stop increase. To verify the continuous operation capability of the robotic arm under closed-loop control, after the actuator is twisted to the targeted angle (Figure 6(d)(iv)),

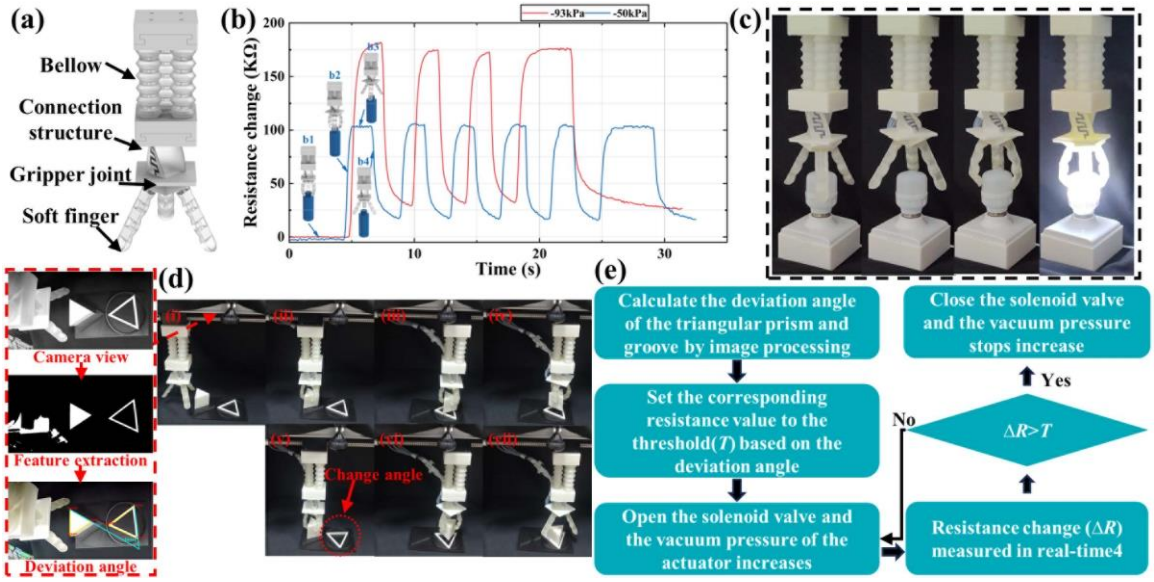

Fig. 6. Soft robotic arm. (a) Structural design of the soft robotic arm. (b) Changes in resistance when actuating the robotic arm in a continuous motion to unscrew a bottle cap. b1: Soft fingers grasp the bottle cap. b2: The twisting actuator rotates to actuate the gripper to twist the bottle cap. b3: The gripper releases the cap. b4: The twist actuator returns to position b1. (c) Using the soft arm to install a light bulb. (d) Under closed-loop control, the robotic arm places the prism into the groove. The full, annotated motion sequence can be found in the Supplementary Video. (e) Closed-loop control diagram.

position of the groove is changed (Figure 6(d)(v)). The experimental result, as shown in Figure 6 (d)(vi) and (d)(vii), demonstrates that the robotic arm can reposition the prism at the new groove location through the closed-loop control algorithm even with a mid-process change in the groove position.

C. *Soft Hexapod Robot*

As shown in Figure 7(a), we design and manufacture a soft hexapod robot to further demonstrate the application of the self-sensing twisting actuator. For the sake of simplicity, we only replaced the head and the left-front twisting actuators with self-sensing twisting actuators for demonstration. There are three twisting actuators on each side of the robot, with clockwise twisting actuators on the left side and counterclockwise twisting actuators on the right side. The vacuum channels of the actuators are controlled by independent solenoid valves. The legs of the robot are covered with sandpaper to increase friction with the ground, promoting the motion of the robot. The robot body includes a control circuit for measuring sensor resistance and transmitting it in real-time to the computer via a Bluetooth module.

Actuating and releasing the actuator leads to forward and backward rotations of the legs, thereby promoting the movement of the hexapod robot. Using different actuation strategies, three gaits are designed for the robot: a walk gait, a left-turn gait, and a right-turn gait (Fig. 7(b)-(d)). As shown in Figure 7(e), the hexapod robot can rotate around a 60cm diameter circle using combinations of the three gaits. The robot can move forward at an average speed of 26.9 mm/s, equivalent to 6.4 times its body length per minute. The turning speed of the robot is 3.5 °/s. By changing the timing of actuating and releasing the twisting actuators, the speed of the hexapod robot can be adjusted.

As shown in Figure 7(b)-(d), when the robot turns left, the left-front actuator remains in the initial state, and there is no change in resistance. When turning right, the left-front actuator completes a rotation cycle in 1.2s. When moving forward, the left-front actuator completes a rotation cycle in 2.4s. Therefore, when turning right, the frequency of resistance change in the actuator is faster (Figure 7(g)). This indicates that monitoring the locomotion modes of the hexapod robot through the change of the resistance is achievable.

Differences in the twisting angles of the actuators result in varying relative movement distances between the legs and the ground during the recovery process. This discrepancy in movement has a direct impact on the overall speed of the robot. We separately actuate the robot forward using -20kPa, -40kPa, and -60kPa pressures, measuring and recording changes in robot resistance and its corresponding movement speeds. During the motion, the changes in robot resistance are depicted in Figure 7(g). When the pressure is -20kPa, the resistance change is approximately 20 KΩ and the movement speed of the robot is 7 mm/s. When the pressure is -60kPa, the resistance change is approximately 105 KΩ, and the movement speed of the robot is 26.1 mm/s. These results indicate that the proposed self-sensing twisting actuators can be used to monitor the movement speed of the hexapod robot.

As shown in Figure 8(a), when a certain level of vacuum pressure is applied, the twisting actuator undergoes further deformation when subjected to external stimuli. Therefore, the self-sensing twisting actuator can also be used for obstacle detection. We integrate the self-sensing twisting actuator into the head of the hexapod robot as a sensing unit for collision detection. We select an acrylic plate as an obstacle, as shown in Figure 8(b). The working mechanism of this device is shown in Figure 8(c). During the robot moving forward, the actuator in the head is in the actuated state, with the sensor continuously providing resistance signals. After colliding with the obstacle, the actuator in the head is stimulated to deform further, and the resistance changes. The actuator is connected to different pressures and the test results are shown in Figure 8(d). The resistance of the actuator increases when the robot encounters the obstacle. The resistance of the actuator changes

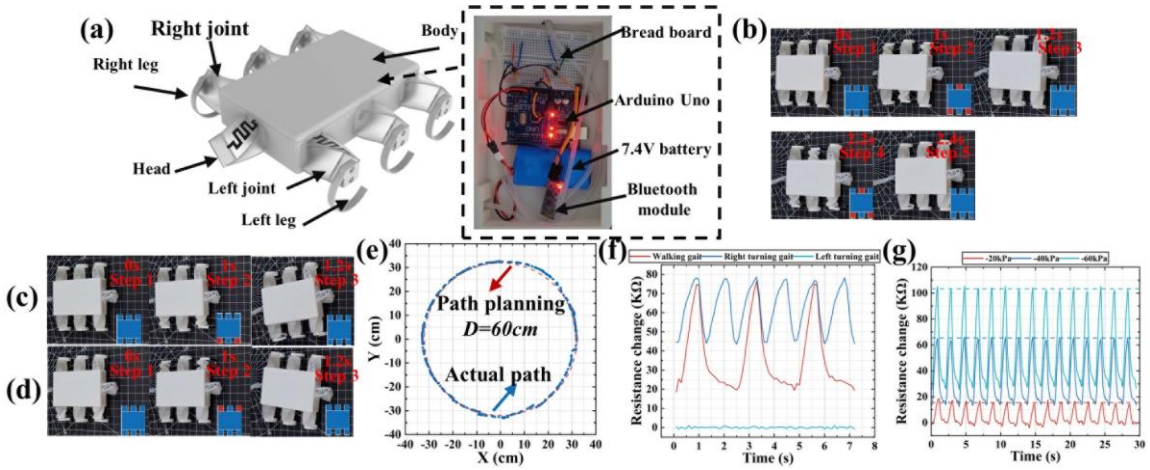

Fig. 7. Soft hexapod robot. (a) Structural design of the hexapod robot. (b) Walk gait. (c) Left-turn gait. (d) Right-turn gait. (e) Combination of three gaits, the hexapod robot can rotate around a circle with a diameter of 60 cm. (f) Different gaits corresponding to the self-sensing twisting actuator resistance change pattern. (g) Changes in the resistance of the actuator when different vacuum pressures are used to actuate the hexapod robot.

differently under different vacuum pressures. Through the resistance feedback of the actuator, we demonstrate that the robot is capable of detecting obstacles and that sensor sensitivity can be adjusted by regulating the vacuum pressure.

IV. Discussion And Conclusion

In this letter, we propose a self-sensing origami-inspired twisting actuator and apply it in several vacuum-powered soft robotic demonstrations. The design based on origami allows the actuator to realize a compound motion of twist and contraction, and the origami structural characteristic improves the responding speed of the soft actuator. By optimizing the design parameters, the impact of snap-through is reduced and the controllability of the actuator is improved. A sensor for a variety of vacuum-powered twisting origami actuators is proposed. The embedding of the sensor does not impede the inherent compliance of the soft actuator and enables position sensing of the actuator through resistance change. Comparison of this work with previous works regarding to origami (especially Kresling origami) inspired actuators for soft robotic applications is given in Table I.

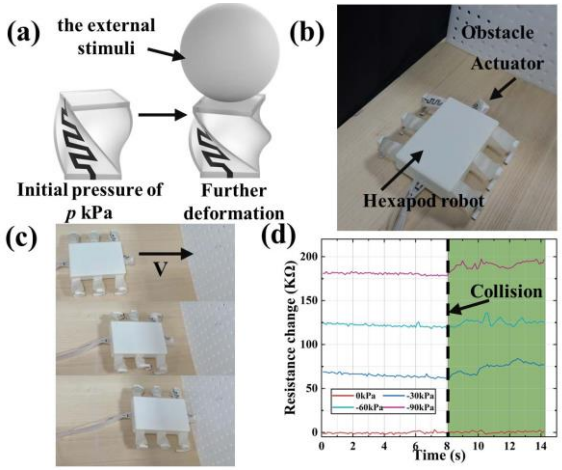

Fig. 8. Obstacle detection of the soft hexapod robot. (a) The twisting actuator is stimulated to deform further. (b) Experimental setup (c) Schematic of collision detection of the hexapod robot. (d) Resistance changes in the hexapod robot when colliding under different initial vacuum pressure conditions.

The proposed self-sensing twisting actuator can be easily adapted to various scenarios as an actuator module. Based on the quadrilateral self-sensing twisting actuator, we fabricate a soft gripper, a soft robotic arm, and a soft hexapod robot. Experimental results demonstrate that the self-sensing twisting actuator performs well not only in grasping and motion, such as detecting object sizes and monitoring the robot gaits but can also serves as a stimulus-detecting device for detecting whether the robot is in a collision or not.

In this paper, we provide an insight for designing self-sensing origami especially twisting origami. The Velostat applied can be easily tailored into desired shape to fit the origami actuator compared to commercially flexible sensors. Except Velostat, other sensing soft materials may also be used for replacement. Moreover, it should be pointed out that the thresholding approach in this study is just one case showing the application based on the actuator's sensory feedback. More applications could be realized, such as:

1) Implement accurate twisting angle feedback control (such as using PI controller [32])

2) Using the resistance-time curves as the training data by adopting the machine learning algorithm [33], we can predict the grasped object in the gripper application and predict the terrain (ground/grass/sand/etc.) in the hexapod application.

In future research, our goals include optimizing the method of combining the sensor with the twisting actuator by placing the sensor inside the curved surface of the actuator to reduce interference from the external environment. Additionally, we plan to improve the control strategies to enhance control precision based on the sensory feedback.

References

[1] D. Rus and M. T. Tolley, "Design, fabrication and control of soft robots," *Nature*, vol. 521, no. 7553, pp. 467-475, 2015.

[2] A. Billard and D. Kragic, "Trends and challenges in robot manipulation," *Science*, vol. 364, no. 6446, 2019.

[3] N. El-Atab *et al.*, "Soft actuators for soft robotic applications: A review," *Adv. Intell. Syst.*, vol. 2, no. 10, 2020.

TABLE I. CPMPARISON OF THIS WORK WITH OTHER ORIGAMI-INSPIRED ACTUATORS FOR SOFT ROBOTIC APPLICATIONS

	Origami design	Motion of origami	Self-sensing involved	Sensing method	Self-sensing for twisting origami	Robotic application
Jiao et al [12]	Kresling twisting tower	Twisting-contraction, twisting-bending	No	NA	No	Soft quadruped robot, soft gripper, pipe-climbing robot, flexible wrist
Ze et al [28]	Kresling twisting tower, magnetic plate	Rolling, flipping, spinning	No	NA	No	Wireless amphibious millirobot
Li et al [21]	Kresling twisting tower	Twisting-contraction	No	NA	No	Soft gripper, versatile robot arm, soft snake robot
Huang et al [31]	Bellows shape	Bending and extension	Yes	Foldable self-inductance sensor	No	Soft gripper, soft jellyfish robot
Dong et al [22]	Bellows shape, Kresling twisting tower	Contraction and bending, twisting-contraction	Yes	Conductive coating	No	Soft amphibious robot (crawling and swimming)
This work	*Kresling twisting tower*	*Twisting-contraction*	*Yes*	*Piezoresistive material*	*Yes*	*Soft gripper, soft robotic arm with twisting wrist, soft hexapod robot*

[4] P. Ohta *et al.*, "Design of a lightweight soft robotic arm using pneumatic artificial muscles and inflatable sleeves," *Soft Robot.*, vol. 5, no. 2, pp. 204-215, 2018.

[5] J. Shintake, V. Cacucciolo, D. Floreano and H. Shea, "Soft robotic grippers," *Adv. Mater.*, vol. 30, no. 29, 2018.

[6] G. Gu *et al.*, "A soft neuroprosthetic hand providing simultaneous myoelectric control and tactile feedback," *Nature Biomed. Eng.*, vol. 5, pp. 1-10, 2021.

[7] E. S. Keneth *et al.*, "Pre-programmed tri-layer electro-thermal actuators composed of shape memory polymer and carbon nanotubes," *Soft Robot.*, vol. 7, no. 2, pp. 123-129, Apr. 2020.

[8] Y. Yang *et al.*, "Novel variable-stiffness robotic fingers with built-in position feedback," *Soft Robot.*, vol. 3, no. 4, pp. 338-352, Nov. 2018.

[9] C. Xiang, J. Guo and S. Davis, "Development of a SMA-fishing-line-mckibben bending actuator," *IEEE Access*, vol. 6, pp. 27183-27189, Apr. 2018.

[10] M. Taghavi, T. Helps and J. Rossiter, "Electro-ribbon actuators and electro-origami robots," *Sci. Robot.*, vol. 3, no. 25, Dec. 2018.

[11] L. Li, W. Ma, Q. Zhang, G. Yuan, H. Li and Y. Tian, "Research on the mechanism of variable stiffness of the twisted and coiled polymer actuator during saturated contraction," *Smart Mater. Struct.*, vol. 29, no. 6, 2020.

[12] Z. Jiao, C. Zhang, W. Wang, M. Pan, H. Yang and J. Zou, "Advanced artificial muscle for flexible material-based reconfigurable soft robots," *Adv. Sci.*, vol. 6, no. 21, 2019.

[13] M. A. Robertson and J. Paik, "New soft robots really suck: Vacuum-powered systems empower diverse capabilities," *Sci. Robot.*, vol. 2, no. 9, Aug. 2017.

[14] C. Tawk, M. In Het Panhuis, G. M. Spinks and G. Alici, "Bioinspired 3D printable soft vacuum actuators for locomotion robots grippers and artificial muscles," *Soft Robot.*, vol. 5, no. 6, pp. 685-694, 2018.

[15] D. Kar, B. George and K. Sridharan, "A review on flexible sensors for soft robotics," *Systems for Printed Flexible Sensors. Bristol U.K.: IOP Publishing 2022*, pp. 1-15.

[16] W. Yan, X. Tian, D. Zhang, Y. Zhou, and Q. Wang, "3D Printing of Stretchable Strain Sensor Based on Continuous Fiber Reinforced Auxetic Structure," *Chinese J. Mech. Eng. Addit. Manuf. Front.*, vol. 2, no. 2, 2023.

[17] B. Jamil, G. Yoo, Y. Choi and H. Rodrigue, "Proprioceptive soft pneumatic gripper for extreme environments using hybrid optical fibers," *IEEE Robot. Autom. Lett.*, vol. 6, no. 4, pp. 8694-8701, Oct. 2021.

[18] Y. Yang and Y. Chen, "Innovative design of embedded pressure and position sensors for soft actuators," *IEEE Robot. Automat. Lett.*, vol. 3, no. 2, pp. 656-663, Apr. 2018.

[19] M. Maselli, D. Zrinscak, V. Magliola and M. Cianchetti, "A piezoresistive flexible sensor to detect soft actuator deformation," *Proc. IEEE 2nd Int. Conf. Soft Robot. (RoboSoft)*, pp. 372-377, Apr. 2019.

[20] T. Jin *et al.*, "Origami-inspired soft actuators for stimulus perception and crawling robot applications," *IEEE Trans. Robot.*, vol. 38, no. 2, pp. 748-764, Apr. 2022.

[21] D. C. Li *et al.*, "Origami-Inspired Soft Twisting Actuator," *Soft Robot.*, vol. 10, no. 2, pp. 395-409, Apr 2023.

[22] H. Dong, H. Yang, S. Ding, T. Li, and H. Yu, "Bioinspired amphibious origami robot with body sensing for multimodal locomotion," *Soft Robot.*, vol. 9, no. 6, pp. 1198-1209, 2022.

[23] J. Liu, G. Ma, Z. Ma and S. Zuo, "Origami-inspired soft-rigid hybrid contraction actuator and its application in pipe-crawling robot," *Smart Mater. Struct.*, vol. 32, no. 6, Jun. 2023.

[24] D. Melancon, A. E. Forte, L. M. Kamp, B. Gorissen, and K. Bertoldi, "Inflatable origami: Multimodal deformation via multistability," *Adv. Funct. Mater.*, vol. 32, no. 35, p. 2201891, 2022.

[25] S. P. M. Babu, R. Das, B. Mazzolai, and A. Rafsanjani, "Programmable inflatable origami," *Proc. IEEE Int. Conf. Soft Robot. (RoboSoft)*, pp. 1-6, 2013.

[26] P. Bhovad, J. Kaufmann and S. Li, "Peristaltic locomotion without digital controllers: Exploiting multi-stability in origami to coordinate robotic motion," *Extreme Mech. Lett.*, vol. 32, 2019.

[27] J. Kaufmann, P. Bhovad and S. Li, "Harnessing the multistability of kresling origami for reconfigurable articulation in soft robotic arms," *Soft Robot.*, vol. 9, no. 2, pp. 212-223, 2022.

[28] Q. Ze, S. Wu, J. Dai, S. Leanza, G. Ikeda, P. C. Yang, G. Iaccarino, and R. R. Zhao, "Spinning-enabled wireless amphibious origami millirobot," *Nat. Commun.*, vol. 13, no. 1, pp. 1–9, 2022.

[29] M. Hopkins, R. Vaidyanathan, and A. H. Mcgregor, "Examination of the performance characteristics of velostat as an in-socket pressure sensor," *IEEE Sensors J.*, vol. 20, no. 13, pp. 6992-7000, Jul. 2020.

[30] J. H. Low, P. M. Khin, and C. H. Yeow, "A pressure-redistributing insole using soft sensors and actuators," *Proc. IEEE Int. Conf. Robot. Autom.*, pp. 2926-2930, 2015.

[31] J. Huang *et al.*, "Modular origami soft robot with the perception of interaction force and body configuration," *Adv. Intell. Syst.*, 2022.

[32] G. Gerboni, A. Diodato, G. Ciuti, M. Cianchetti and A. Menciassi, "Feedback control of soft robot actuators via commercial flex bend sensors", *IEEE/ASME Trans. Mechatron.*, vol. 22, no. 4, pp. 1881-1888, Aug. 2017.

[33] T. G. Thuruthel, B. Shih, C. Laschi and M. T. Tolley, "Soft robot perception using embedded soft sensors and recurrent neural networks", *Sci. Robot.*, vol. 4, no. 26, 2019.